

## Two high-temperature paraelectric phases in $\text{Sr}_{0.85}\text{Bi}_{2.1}\text{Ta}_2\text{O}_9$

C. H. Hervoches, J. T. S. Irvine, and P. Lightfoot\*

*School of Chemistry, University of St. Andrews, St. Andrews, Fife KY16 9ST, United Kingdom*

(Received 16 March 2001; published 22 August 2001)

$\text{Sr}_{0.85}\text{Bi}_{2.1}\text{Ta}_2\text{O}_9$  is shown, by Rietveld refinement of powder neutron-diffraction data, to undergo two phase transitions at elevated temperature. The low-temperature ferroelectric phase (space group  $A2_1am$ ) transforms to a paraelectric phase ( $Amam$ ) at  $T_c \sim 375^\circ\text{C}$ . This phase does not transform to the expected tetragonal phase ( $I4/mmm$ ) until  $T \sim 550^\circ\text{C}$ . The transition from  $A2_1am$  to  $Amam$  involves not only loss of the displacive mode along the polar  $a$  axis, but also loss of a  $\text{TaO}_6$  octahedral tilt mode around the  $c$  axis.

DOI: 10.1103/PhysRevB.64.100102

PACS number(s): 77.84.Dy, 77.80.Bh, 61.66.Fn, 61.12.Ld

The Aurivillius family of layered bismuth-containing oxides encompasses many ferroelectric materials, a fact which has been known since the pioneering work of Smolenskii<sup>1</sup> and Subbarao<sup>2</sup> forty years ago. In recent years, considerable interest in these materials has been rekindled due to the observation of fatigue-free behavior and low coercive field in ferroelectric thin films of  $\text{SrBi}_2\text{Ta}_2\text{O}_9$  (SBT) and related materials.<sup>3</sup> This makes SBT currently the material of choice for potential applications in ferroelectric random access memories (FeRAM's). The properties of SBT itself may be tailored subtly by altering the stoichiometry to a slightly Bi excess composition, nominally  $\text{Sr}_{0.8}\text{Bi}_{2.2}\text{Ta}_2\text{O}_9$ ,<sup>4</sup> which shows a much larger spontaneous polarization ( $\sim 10 \mu\text{Ccm}^{-2}$ ) and higher  $T_c$  ( $400^\circ\text{C}$ ) than that of stoichiometric SBT ( $5.8 \mu\text{Ccm}^{-2}$  and  $335^\circ\text{C}$ , respectively). In addition to the single crystal x-ray study of SBT,<sup>5</sup> detailed crystallographic characterization of both SBT and an off-stoichiometric composition,  $\text{Sr}_{0.85}\text{Bi}_{2.1}\text{Ta}_2\text{O}_9$ , in their room-temperature ferroelectric phases, has recently been carried out by Shimakawa *et al.*,<sup>6</sup> using powder neutron diffraction (PND). This technique is considerably more suitable to the study of these materials in bulk polycrystalline form than powder x-ray diffraction (PXRD) due to the smaller variation in the scattering factors for the elements involved; i.e., x-ray scattering is too dominated by the scattering of the heavy atoms to allow precise and meaningful location of oxygen atom positions. Until now, however, powder neutron-diffraction techniques have only been applied to the study of the ferro- to paraelectric phase transition in one Aurivillius phase, viz.  $\text{Bi}_4\text{Ti}_3\text{O}_{12}$ .<sup>7</sup> Recent reports<sup>8</sup> of the thermal behavior of both SBT and  $\text{Sr}_{0.85}\text{Bi}_{2.1}\text{Ta}_2\text{O}_9$ , however, have suggested that the two compositions may undergo a differing sequence of phase transitions at elevated temperature, and a very recent variable temperature PXD study<sup>9</sup> has proposed an intermediate phase may exist for  $\text{Sr}_{0.85}\text{Bi}_{2.1}\text{Ta}_2\text{O}_9$  in the region  $237^\circ\text{C} < T < 397^\circ\text{C}$ , based on anomalous changes in lattice parameters vs temperature. That study also proposed a model for the high-temperature phase (at  $477^\circ\text{C}$ ) in space group  $I4/mmm$ , which is the "expected" highest symmetry structure for an Aurivillius phase, and has been confirmed in the case of  $\text{Bi}_4\text{Ti}_3\text{O}_{12}$  by our own PND analysis.<sup>7</sup> We have now carried out our own variable temperature PND study of  $\text{Sr}_{0.85}\text{Bi}_{2.1}\text{Ta}_2\text{O}_9$  and confirm that there are, indeed, two high-temperature phase transitions, in agreement with the hypothesis of Onodera *et al.* In detail, however, our present results

differ dramatically from those of the Onodera, determined by PXD and provide, we believe, a much more precise insight into the structural behavior of this important material.

A 10 g polycrystalline sample of  $\text{Sr}_{0.85}\text{Bi}_{2.1}\text{Ta}_2\text{O}_9$  suitable for PND was prepared by traditional solid-state reaction. Stoichiometric quantities of  $\text{Bi}_2\text{O}_3$ ,  $\text{SrCO}_3$ , and  $\text{Ta}_2\text{O}_5$  were mixed, ground, and heated together at  $850^\circ\text{C}$  for 24 h, followed by two firings of 24 h at  $1000^\circ\text{C}$ . Preliminary PXD on a Stoe STADI/P powder diffractometer, revealed that the sample was phase pure. Powder neutron-diffraction data were collected on the high-resolution powder diffractometer HRDP at the CLRC ISIS Facility, U.K. Data were collected in a thin-walled cylindrical vanadium can at temperatures of 110, 200, 250, 300, 350, 400, 450, 500, and  $550^\circ\text{C}$ , each

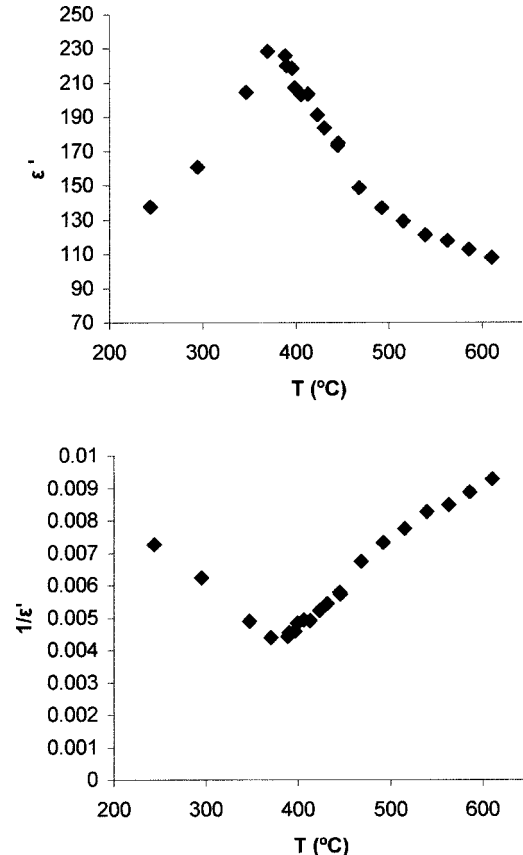


FIG. 1. Dielectric constant vs  $T$  showing  $T_c \sim 375^\circ\text{C}$ .

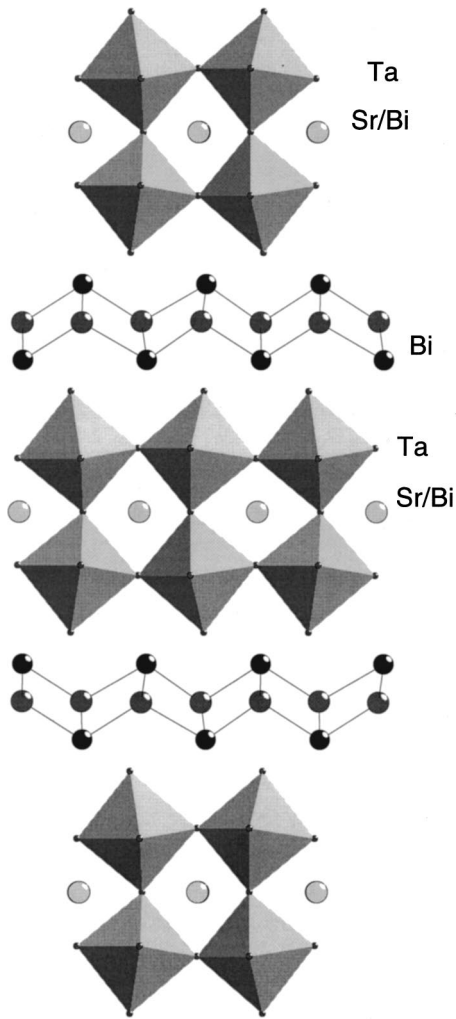


FIG. 2. Crystal structure of the  $A2_1am$  ferroelectric phase of  $Sr_{0.85}Bi_{2.1}Ta_2O_9$  at  $110^\circ C$ .

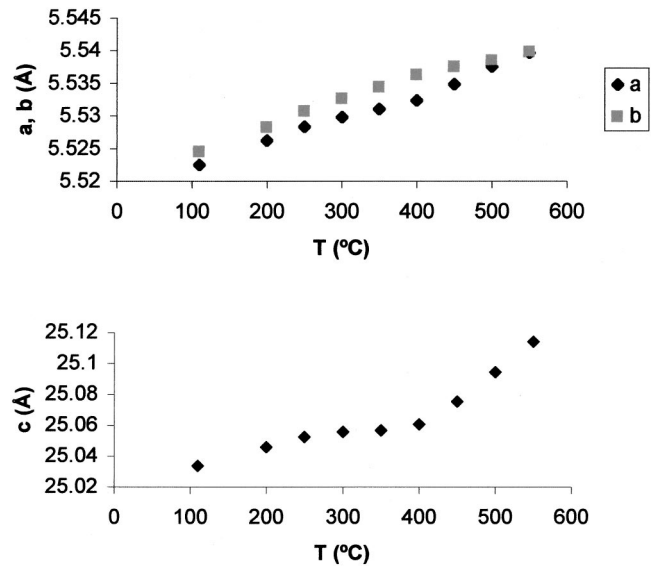


FIG. 3. Lattice parameters for  $Sr_{0.85}Bi_{2.1}Ta_2O_9$  as a function of temperature, determined from Rietveld refinement of powder neutron-diffraction data.

data collection lasting approximately 2 h. The HRPD instrument operates in time-of-flight mode, with fixed detector banks. Only the data from the high-resolution “backscattering” banks ( $2\theta \sim 168^\circ$ ) were used for subsequent Rietveld analysis using the GSAS suite.<sup>10</sup> All the refinements were carried out using a data range  $0.65 < d < 2.5 \text{ \AA}$ . Dielectric data were collected by a.c. impedance spectroscopy using a Solartron 1255 Frequency Response Analyser with a 1287 Electrochemical Interface. Measurements were performed using an ac amplitude of 20 mV over the frequency range 100 mHz–1 MHz.

Impedance data showed a single Debye-type arc. The response indicated a highly resistive electronic component in parallel with a temperature-dependent dielectric component. The dielectric constant increases with temperature up to  $375^\circ C$  and then decreases sharply as temperature is further

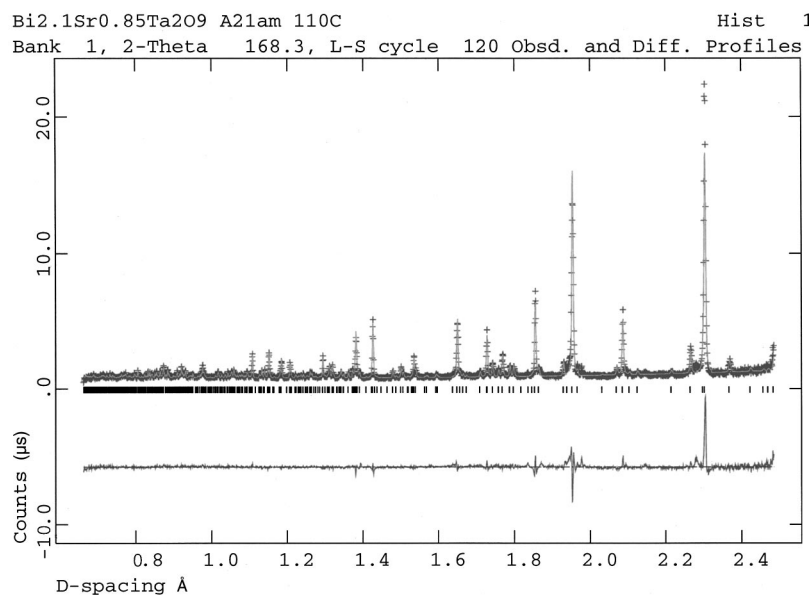


FIG. 4. Final Rietveld profile for  $Sr_{0.85}Bi_{2.1}Ta_2O_9$  at  $110^\circ C$  ( $A2_1am$ ).

TABLE I. Refined structural parameters for  $\text{Sr}_{0.85}\text{Bi}_{2.1}\text{Ta}_2\text{O}_9$  at 110 °C, space group  $A2_1am$ ,  $a=5.5225(2)$  Å,  $b=5.5246(2)$  Å, and  $c=25.0338(6)$  Å.

Atom	$x$	$y$	$z$	$U_{iso}$ (x100)
Sr(1) <sup>a</sup>	0 <sup>b</sup>	0.2472(15)	0	1.6(1)
Bi(1)	0.4555(16)	0.7687(11)	0.20010(14)	2.6(1)
Ta(1)	0.5138(20)	0.7456(14)	0.41496(14)	1.00(8)
O(1)	0.5187(27)	0.2985(21)	0	1.6(2)
O(2)	0.5137(22)	0.6917(15)	0.34137(22)	2.3(2)
O(3)	0.7295(22)	0.9983(18)	0.25072(33)	1.5(1)
O(4)	0.7524(26)	0.9862(17)	0.07026(22)	1.8(2)
O(5)	0.7882(23)	0.9709(15)	0.58381(23)	1.5(2)

<sup>a</sup>Occupancy of site: 0.85 Sr/0.1 Bi.

<sup>b</sup>Fixed to define origin of polar axis.

TABLE II. Refined structural parameters for  $\text{Sr}_{0.85}\text{Bi}_{2.1}\text{Ta}_2\text{O}_9$  at 450 °C, space group  $Amm$ ,  $a=5.5350(2)$  Å,  $b=5.5376(2)$  Å, and  $c=25.0755(5)$  Å.

Atom	$x$	$y$	$z$	$U_{iso}$ (x100)
Sr(1) <sup>a</sup>	0.25 <sup>b</sup>	0.2401(18)	0	3.1(1)
Bi(1)	0.75	0.7605(13)	0.20015(13)	4.9(1)
Ta(1)	0.75	0.7485(14)	0.41454(12)	1.75(7)
O(1)	0.75	0.2784(26)	0	3.9(2)
O(2)	0.75	0.6954(16)	0.34141(22)	4.0(2)
O(3)	0	0	0.25010(39)	2.5(1)
O(4)	0	0	0.07220(24)	3.1(2)
O(5)	0	0	0.58214(25)	3.8(3)

<sup>a</sup>Occupancy of site 0.85 Sr/0.1 Bi.

<sup>b</sup>There is a shift of  $\Delta x=0.25$  between the settings of space groups  $A2_1am$  and  $Amm$ .

TABLE III. Refined structural parameters for  $\text{Sr}_{0.85}\text{Bi}_{2.1}\text{Ta}_2\text{O}_9$  at 550 °C, space group  $I4/mmm$ ,  $a=3.91721(6)$  Å and  $c=25.1142(5)$  Å.

Atom	$x$	$y$	$z$	$U_{11}$ (x100) <sup>b</sup>	$U_{22}$ (x100)	$U_{33}$ (x100)
Sr(1) <sup>a</sup>	0.5	0.5	0	2.9(2)	2.9(2)	4.4(4)
Bi(1)	0.5	0.5	0.20019(13)	5.6(2)	5.6(2)	5.0(2)
Ta(1)	0	0	0.41442(14)	1.5(1)	1.5(1)	3.1(2)
O(1)	0	0	0	5.5(3)	5.5(3)	1.6(4)
O(2)	0	0	0.34069(21)	10.0(3)	10.0(3)	2.6(3)
O(3)	0	0.5	0.25	2.8(2)	2.8(2)	3.2(2)
O(4)	0	0.5	0.07723(11)	4.7(2)	1.0(2)	6.5(2)

<sup>a</sup>Occupancy of site: 0.85 Sr/0.1 Bi.

<sup>b</sup>Anisotropy refinement carried out.

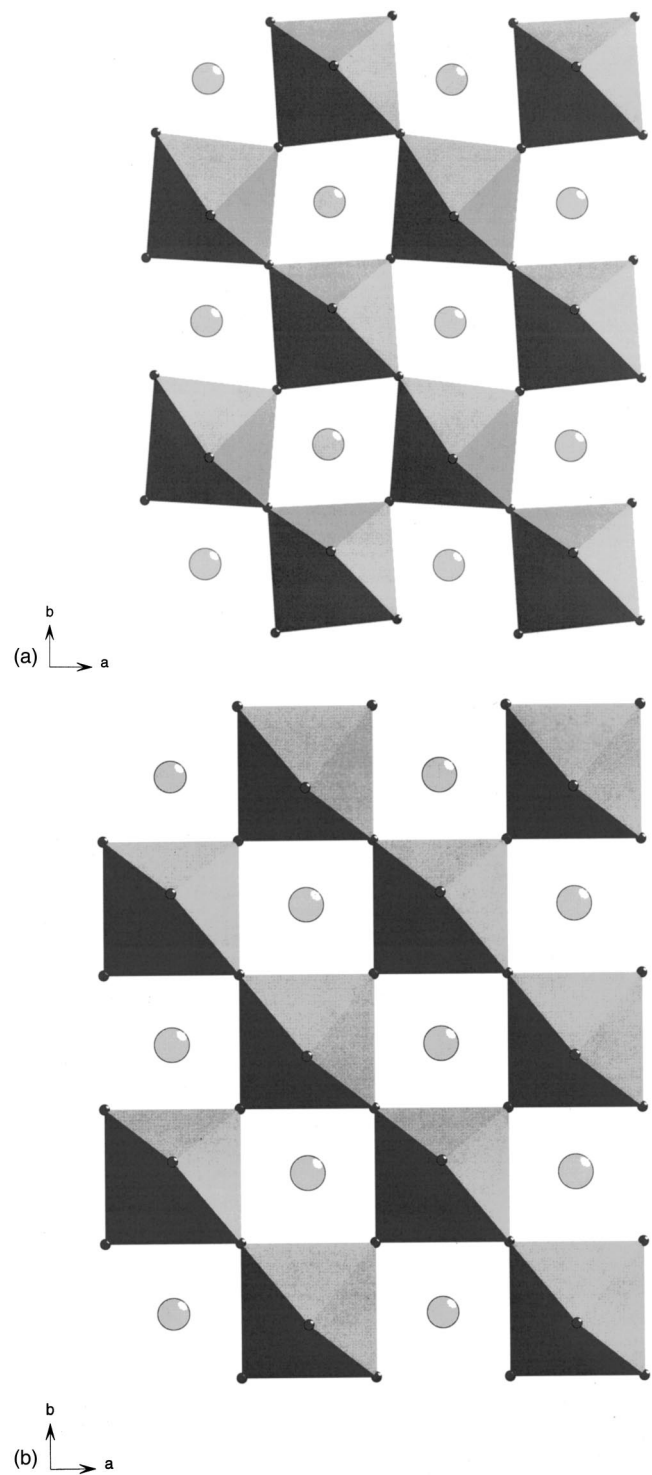


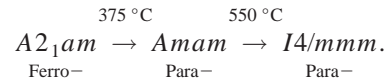
FIG. 5. Projections of one perovskite unit along the  $c$  axis showing loss of the octahedral tilt mode around  $c$ : (a)  $A2_1am$ , (b)  $Amm$ .

increased (Fig. 1). This shows clear evidence of a ferroelectric to paraelectric transition at  $T_c \sim 375$  °C.

Refinement of the PND data at 110 °C was carried out using the model of Shimakawa *et al.* in space group  $A2_1am$ .<sup>6</sup> The crystal structure in this phase is shown in Fig. 2. We note that in stoichiometric  $\text{SrBi}_2\text{Nb}_2\text{O}_9$  there is partial

disorder of the Sr/Bi cations over the two sites (i.e., the  $[\text{Bi}_2\text{O}_2]$  layer site and the perovskite  $A$  site).<sup>11</sup> However, in this case, neither our PXD data nor the PND data provided any evidence for a similar disorder, presumably due, in part, to the Bi excess nature of this composition. The occupancies of these sites were therefore kept fixed throughout all subsequent refinements. High quality Rietveld fits were obtained in this model for all temperatures up to 550 °C. At this stage it became apparent that the transition to the “parent” phase in  $I4/mmm$  had occurred. Therefore, the refinement at 550 °C was also carried out in this space group, with a high quality fit again being obtained (Goodness-of-fit indices  $\chi^2 = 3.49(R_{wp} = 6.4\%)$  and  $\chi^2 = 3.17(R_{wp} = 6.1\%)$  for the  $A2_1am$  and  $I4/mmm$  refinements, respectively). At this stage, the thermal evolution of the lattice parameters was plotted (Fig. 3). An unexpected feature can now be seen, providing unambiguous evidence for an intermediate phase transition, rather than a transition directly from  $A2_1am$  to  $I4/mmm$ . The orthorhombicity  $[2(b-a)/(b+a)]$  of the sample actually *increases* in the range  $250^\circ\text{C} < T < 375^\circ\text{C}$ , with the maximum orthorhombicity coinciding with a change of slope in the  $c$  parameter vs  $T$ , at  $\sim 375^\circ\text{C}$ . This correlates with a measured  $T_c$  for the present sample of  $375^\circ\text{C}$ . Together, these data confirm the existence of an intermediate phase in the region  $375 < T < 550^\circ\text{C}$ . Careful scrutiny of the neutron powder diffraction data at  $450^\circ\text{C}$  suggested that there had been no change in lattice type, for example to a F-centred orthorhombic system, which has been suggested as a possible intermediate phase in some Aurivillius systems. For example, the presence of reflections 233, 1210, and 033 confirm the  $A$ -centered nature of the lattice. Therefore, a refinement of the  $450^\circ\text{C}$  data was performed in the centrosymmetric space group  $Amam$ , compatible with the observed systematic absences, and the simplest supergroup of  $A2_1am$ . [We note that the presence of the 033 reflection also negates the possibility of the alternative space group  $Abam$ .] As a comparative test of the validity of this model,

we also applied it to the data at  $110^\circ\text{C}$ . The resulting  $\chi^2/R_{wp}$  values for the four Rietveld refinements were:  $110^\circ\text{C}$  –  $5.01/7.6\%$  ( $A2_1am$ ),  $7.06/9.1\%$  ( $Amam$ );  $450^\circ\text{C}$  –  $3.55/6.4\%$  ( $A2_1am$ ),  $3.62/6.5\%$  ( $Amam$ ) for 39 and 29 variables in the case of  $A2_1am$  and  $Amam$ , respectively. This analysis shows unambiguously that the  $Amam$  model for the intermediate phase is valid, as the observed very slight improvement in  $\chi^2$  in going to the lower symmetry phase, at  $450^\circ\text{C}$  can be taken as insignificant. The final Rietveld fit for the  $A2_1am$  model, at  $110^\circ\text{C}$ , is given in Fig. 4. We have shown, therefore, that the following series of phase transitions occurs for  $\text{Sr}_{0.85}\text{Bi}_{2.1}\text{Ta}_2\text{O}_9$ :



Final refined crystallographic parameters for the three phases are given in Tables I–III. The structure of  $\text{Sr}_{0.85}\text{Bi}_{2.1}\text{Ta}_2\text{O}_9$  in the ferroelectric  $A2_1am$  phase given in Fig. 1. The difference between the  $A2_1am$  and  $Amam$  structures is firstly that the displacive mode along the polar axis ( $a$ ) is lost and, secondly, that a rotational mode of the  $\text{TaO}_6$  octahedra, around the  $c$  axis, of the perovskite unit is also lost (in space group  $Abam$  this rotational mode would not be lost). This is best seen by a comparison of the  $c$ -axis projections one octahedral layer of the structures (Fig. 5). The reasons for this unexpected behavior are not yet understood in detail, but they may depend subtly on the nature of the individual cation sites within the structure, and the number of perovskite layers present. A future comparison with related Aurivillius phases  $\text{SrBi}_2\text{Nb}_2\text{O}_9$ ,  $\text{Bi}_4\text{Ti}_3\text{O}_{12}$  and  $\text{SrBi}_4\text{Ti}_4\text{O}_{15}$ , having 2, 3, and 4 perovskite layers, respectively, is planned; the latter two do not appear to show an intermediate paraelectric phase.<sup>7,12</sup>

We would like to thank EPSRC for financial support (to C.H.H.) and for provision of neutron-diffraction facilities at ISIS. We thank Dr. K. S. Knight and Dr. R. M. Ibberson for help in the neutron data collection.

\*Corresponding author. Email address: pl@st-and.ac.uk

<sup>1</sup>G. A. Smolenskii, V. A. Isupov, and A. I. Agranovskaya, *Sov. Phys. Solid State* **3**, 651 (1959).

<sup>2</sup>E. C. Subbarao, *J. Phys. Chem. Solids* **23**, 665 (1962).

<sup>3</sup>C. A. P. de Araujo, J. D. Cuchlaro, L. D. McMillan, M. Scott, and J. F. Scott, *Nature (London)* **374**, 627 (1995).

<sup>4</sup>T. Noguchi, T. Hase, and Y. Miyasaka, *Jpn. J. Appl. Phys., Part 1* **35**, 4900 (1996).

<sup>5</sup>A. D. Rae, J. G. Thompson, and R. L. Withers, *Acta Crystallogr., Sect. B: Struct. Sci.* **48**, 418 (1992).

<sup>6</sup>Y. Shimakawa, Y. Kubo, Y. Nakagawa, T. Kamiyama, H. Asano,

and F. Izumi, *Appl. Phys. Lett.* **74**, 1904 (1999).

<sup>7</sup>C. H. Hervoches and P. Lightfoot, *Chem. Mater.* **11**, 3359 (1999).

<sup>8</sup>A. Onodera, K. Yoshio, C. C. Myint, S. Kojima, H. Yamashita, and T. Takama, *Jpn. J. Appl. Phys., Part 1* **38**, 5683 (1999).

<sup>9</sup>A. Onodera, T. Kubo, K. Yoshio, S. Kojima, H. Yamashita, and T. Takama, *Jpn. J. Appl. Phys., Part 1* **39**, 5711 (2000).

<sup>10</sup>A. C. Larson and R. B. von Dreele, Los Alamos National Laboratory Report No. LA-UR-86-748, 1987 (unpublished).

<sup>11</sup>S. M. Blake, M. J. Falconer, M. McCreedy, and P. Lightfoot, *J. Mater. Chem.* **7**, 1609 (1997).

<sup>12</sup>C. H. Hervoches and P. Lightfoot (unpublished).